Exogenous carbon turnover within the soil food web strengthens soil carbon sequestration through microbial necromass accumulation

Kou, X.; Morriën, E.; Tian, Y.; Zhang, X.; Lu, C.; Xie, H.; Liang, W.; Li, Q.; Liang, C.

DOI
10.1111/gcb.16749

Publication date
2023

Document Version
Final published version

Published in
Global Change Biology

Received: 2 December 2022 | Accepted: 25 April 2023

DOI: 10.1111/gcb.16749

Global Change Biology WILEY

RESEARCH ARTICLE

Exogenous carbon turnover within the soil food web strengthens soil carbon sequestration through microbial necromass accumulation

Xinchang Kou[1,2] | Elly Morriën[3] | Yijia Tian[1,4] | Xiaoke Zhang[1] | Caiyan Lu[1] | Hongtu Xie[1] | Wenju Liang[1] | Qi Li[1] | Chao Liang[1]

[1]Institute of Applied Ecology, Chinese Academy of Sciences, Shenyang, China

[2]Key Laboratory of Geographical Processes and Ecological Security in Changbai Mountains, Ministry of Education, School of Geographical Sciences, Northeast Normal University, Changchun, China

[3]Institute for Biodiversity and Ecosystem Dynamics, Ecosystem and Landscape Dynamics Department (IBED-ELD), University of Amsterdam, Amsterdam, The Netherlands

[4]University of Chinese Academy of Sciences, Beijing, China

Correspondence
Xiaoke Zhang and Qi Li, Institute of Applied Ecology, Chinese Academy of Sciences, P. O. Box 417, Shenyang 110016, China.
Email: zxk@iae.ac.cn; liq@iae.ac.cn

Funding information
National Key Research and Development Plan, China, Grant/Award Number: 2022YFD1500202 and 2022YFD1500601; the Strategic Priority Research Program of the Chinese Academy of Sciences, Grant/Award Number: XDA28020202 and XDA28010102; the National Natural Science Foundation of China, Grant/Award Number: U22A20501 and 41977054; the Science and Technology Research Project of the Education Department of Jilin Province, Grant/Award Number: JJKH20221164KJ; the K.C. Wong Education Foundation, Grant/Award Number: GJTD-2019-10; Major Program of Institute of Applied Ecology, Chinese Academy of Science, Grant/Award Number: IAEMP202201

Abstract

Exogenous carbon turnover within soil food web is important in determining the trade-offs between soil organic carbon (SOC) storage and carbon emission. However, it remains largely unknown how soil food web influences carbon sequestration through mediating the dual roles of microbes as decomposers and contributors, hindering our ability to develop policies for soil carbon management. Here, we conducted a ^{13}C-labeled straw experiment to demonstrate how soil food web regulated the residing microbes to influence the soil carbon transformation and stabilization process after 11 years of no-tillage. Our work demonstrated that soil fauna, as a "temporary storage container," indirectly influenced the SOC transformation processes and mediated the SOC sequestration through feeding on soil microbes. Soil biota communities acted as both drivers of and contributors to SOC cycling, with 32.0% of exogenous carbon being stabilizing in the form of microbial necromass as "new" carbon. Additionally, the proportion of mineral-associated organic carbon and particulate organic carbon showed that the "renewal effect" driven by the soil food web promoted the SOC to be more stable. Our study clearly illustrated that soil food web regulated the turnover of exogenous carbon inputs by and mediated soil carbon sequestration through microbial necromass accumulation.

KEYWORDS
carbon sequestration, isotope tracing, microbial necromass, soil fauna, soil food web, trophic cascade

1 | INTRODUCTION

The soil organic carbon (SOC) pool contains approximately three times as much carbon as the atmosphere (Jackson et al., 2017; Liang, 2020; Schmidt et al., 2015; Stockmann et al., 2013), and even slight changes in it will have a significant impact on the carbon balance (Bradford et al., 2016; Lehmann et al., 2020). Straw return practices have the potential to increase soil carbon stocks and stimulate soil biota communities to enhance carbon sequestration (Luo et al., 2020). As well known, the effectiveness of straw returns practices and the amount of SOC accumulation not only depends on the quantity and quality of organic matter inputs, but also relies highly on the activities of soil food web (Bhattacharyya et al., 2022; Garcia-Palacios et al., 2016; Pausch et al., 2016; Torri et al., 2014).

Over the last decade, it is generally accepted that microorganisms are regarded as the primary processors of SOC decomposition and formation (Domeignoz-Horta et al., 2020; Mitchell et al., 2020; Schimel & Schaeffer, 2012). Microorganisms play a dual role in SOC cycling by two contrasting mechanisms: the reduction of SOC stock through decomposition and the increase through the formation of microbial biomass and stabilization of its residues (Liang et al., 2017). The recent conceptual framework of soil "microbial carbon pump" (MCP) denotes that microbial biosynthesized products can result in a significant net contribution of microbial-derived carbon to the long-lasting soil carbon pool (Liang et al., 2017). This occurs through microbial anabolism that contributes to the accumulation of microbial necromass, which can later become stabilized through interactions with soil minerals and aggregates, as known as the entombing effect. The MCP-driven microbial entombing effect leads to the deposition of microbial necromass on soil mineral surfaces or within soil aggregates, which in turn accelerates soil carbon sequestration. However, despite substantial evidence supporting the importance of microbial necromass for stable SOC sequestration, research has often neglected the regulatory role of the soil food web (Ni et al., 2021; Wang, An, et al., 2021; Wang, Qu, et al., 2021; Zhu et al., 2021).

Since microorganisms are inevitably regulated by microfauna and mesofauna at higher trophic levels, both consumers and predators within soil food web might play key roles in regulating carbon stabilization or destabilization in soils (de Castro et al., 2021; Garcia-Palacios et al., 2016) (Figure 1). Therefore, the potential influence of soil fauna at higher trophic levels on SOC formation processes should not be neglected (Angst et al., 2022; Thakur & Geisen, 2019). Despite recent research focusing increasingly on the role of soil biota, identifying the impact mechanism of soil food webs on the transformation process of SOC remains challenging. Moreover, the SOC pool can be separated into active and stable carbon pools or different functional components by its nature, for example, particulate organic carbon (POC) and mineral-associated organic carbon (MAOC), which are of great importance for understanding the persistence of SOC (Cotrufo et al., 2013; Lavallee et al., 2020). Thus, to comprehensively explore the influence of soil food web on soil carbon cycling, it is important to integrate labile and non-labile biological fixation carbon for facilitating the understanding of how soil food web controls over the SOC renewal and sequestration process.

Soil food webs, as regulators of the decomposition pathway, can influence nutrient availability and carbon cycling in a myriad of ways, such as through the regulation of the quantity and quality of carbon resources, or even through the direct influences on microbial populations (Bardgett & Wardle, 2010; Thakur & Geisen, 2019). Direct feeding relationships between fungi and fungivores, or between bacteria and bacterivores, can promote carbon fluxes in the predation channel (Crowther et al., 2015; Gan et al., 2018; Soong et al., 2016).

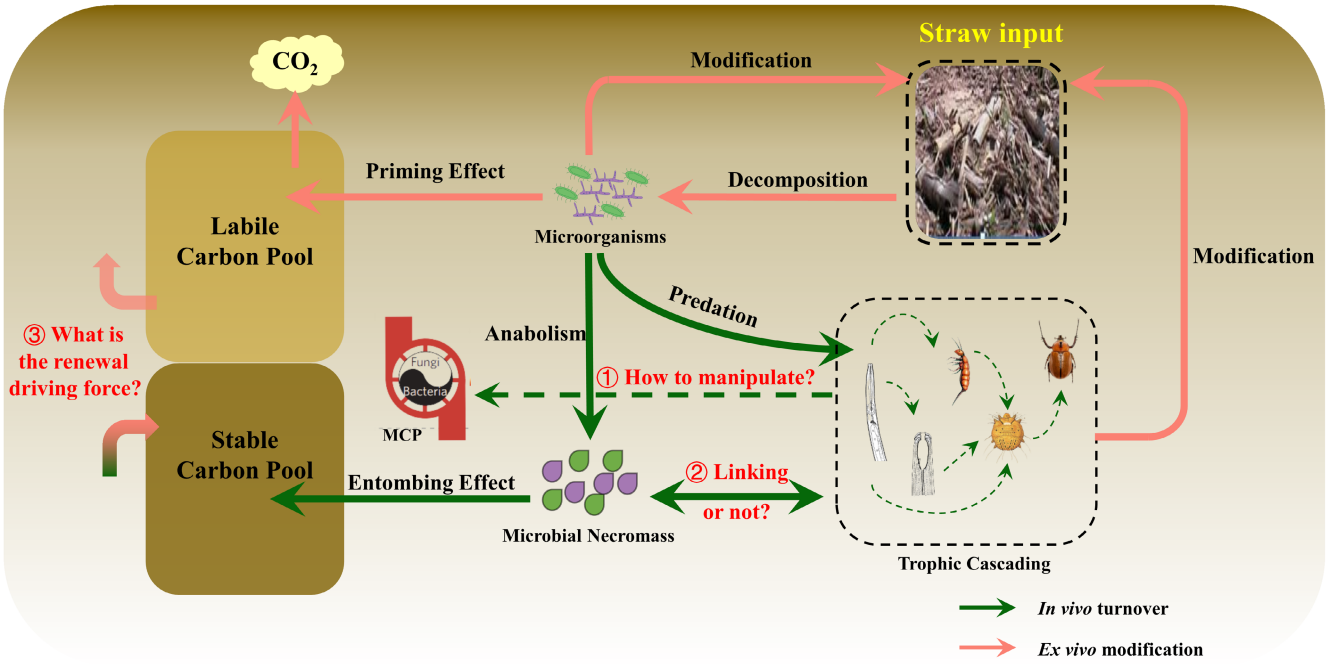

FIGURE 1 Conceptual scheme on the regulation process of soil food web to soil carbon pool renewal. [Colour figure can be viewed at wileyonlinelibrary.com]

Thus, we generally infer that soil fauna at higher trophic levels can manipulate soil carbon cycling process through predation in soil food web (Grandy et al., 2016; Kastner & Miltner, 2018; Sackeet et al., 2010). Previous studies have also pointed out that only small amounts of ^{13}C in isotope enrichment experiments were transferred to higher trophic levels (Pausch et al., 2016) and shaped carbon flux in a binary link between prey and predator (Richter et al., 2019). However, the role that soil food web plays in manipulating the MCP is essentially unknown (Figure 1).

To close this knowledge gap, we conducted an isotope tracing experiment with ^{13}C-labeled maize residue on the basis of a long-term field straw mulching experiment. Our objective is to reveal how biological interactions within soil food web mediate soil microbes and their necromass accumulation, and how they motivate SOC renewal processes by manipulating the MCP. We hypothesize that (i) the soil food web, as both decomposers and drivers, makes important contributions to exogenous carbon renewal and turnover; (ii) the formation process of SOC is not only tightly related to microbes and microbial necromass, but is also regulated by the consumers of microbes, that is, soil fauna; and (iii) the SOC renewal process mediates by soil food web will affect the persistence of SOC by changing its fraction.

2 | MATERIALS AND METHODS

2.1 | Soil sampling in the field manipulation experiment

The straw mulching experiment has been established in 2007 at the Conservation Tillage Research and Development Station of the Chinese Academy of Sciences located in Jilin Province of northeastern China (43°19′N, 124°14′E) (Jiang et al., 2021). The field experimental design was described in detail in Kou et al. (2020). The three application treatments were with 33% of total harvest straw (2475 kg ha^{-1}, NT33), with 67% of total harvest straw (4950 kg ha^{-1}, NT67) and 100% straw return (7500 kg ha^{-1}, NT100) for each year (Kou et al., 2020; Luo et al., 2021). In each plot, eight soil cores were randomly collected with a 2.5 cm diameter auger at a depth of 0–10 cm from the maize field with long-term straw return at the ripening stage of maize and then uniformly mixed as a composite sample in 2018. At this stage, the activity of soil fauna was relatively stable due to the high decomposition of straw. The fresh samples were stored individually in plastic bags and kept at 4°C in a refrigerator.

2.2 | Soil incubation experiment

Soil incubation experiment was conducted in 2018 on the basis of field experiment. Fresh soils obtained from the field were passed through a 6-mm sieve (little disturbance to soil microfauna and mesofauna) and visible stones, roots, and plant residues were manually removed, and then stored at 4°C for the incubation experiment. We used axenic glass jars (750 mL) as incubation containers filled with 500 g of uniformly mixed soil. Then, preincubation was carried out at 25°C in the dark for 7 days prior to maize residue addition in order to allow soil fauna to acclimate to the laboratory incubation condition (Kou et al., 2020). In all containers, water content was artificially adjusted to 60% of water-holding capacity with deionized water and maintained during the incubation process by weighing the jars every 2 days. After the preincubation, the labeled ^{13}C straw was added according to the actual amount application in the field. Correspondingly, the isotope-^{13}C labeled residue (^{13}C maize residue, 97 atom % ^{13}C, No U-60501, Wageningen University, The Netherlands) were applied homogeneously on the soil surface with 0.3, 0.6, and 0.9 g, which corresponded, respectively, to the 33%, 67%, and 100% straw mulching treatments. Meanwhile, the controls without residue addition were set up at the same time. After an incubation of 7, 27, 54, and 84 days, destructive sampling was conducted. In total, there were 96 samples ((3 labeled + 3 control treatments) × 4 replicates × 4 harvests). Each soil sample was then thoroughly homogenized for the further extraction of microorganisms, nematodes, and other mesofauna.

2.3 | Soil property and soil microbe analysis

The SOC was determined by an automatic elemental analyzer (Elemental Analyzer System Vario MACRO cube, Germany), and the values of ^{13}C enrichment in the SOC were measured by a MAT 253 isotope ratio mass spectrometer (EA-IRMS, Elementanalysis-Stable100 Isotope Ratio Mass Spectrometer, Germany). The analysis of POC and MAOC was based on the method of particle density grouping (Cotrufo et al., 2019; Lavallee et al., 2020). The separated components were dried at 55°C, and then, the PO^{13}C and MAO^{13}C were measured by a MAT 253 isotope ratio mass spectrometer. Released CO_2 was trapped in small bottles with 10 mL of 1 M NaOH placed in the incubation bottle which was closed air-tight for 3 h. Excess 1 M $BaCl_2$ was added to precipitate $BaCO_3$ and the precipitate was transferred to a 50 mL centrifuge tube and added deionized water, and then centrifuged for 2 min at 2500 rpm. The $BaCO_3$ pellets were dried at 80°C for 48 h and stored for $\delta^{13}C$ analysis by a MAT 253 isotope ratio mass spectrometer (Sven et al., 2007).

Soil microbial community composition and biomass were characterized using phospholipid fatty acid analysis (PLFA) according to Bossio et al. (1998). Briefly, lipids from 6 g of fresh soil were extracted with a buffer that consisted of a mixture of citrate–chloroform–methanol (0.8:1:2). Solid-phase extraction columns (Supelco Inc.) were used to separate polar lipids from neutral lipids and glycolipids. The produced fatty acid methyl esters (FAMEs) were extracted in hexane and dried under N_2. Samples were first analyzed with an Agilent Technologies 7890B with MIDI peak identification software (Version 4.5; MIDI Inc.), and then dried under N_2 once again for further ^{13}C enrichment determination. The isotope ratio of individual FAME was measured with a GC-C-IRMS. Each kind of

FAME measured by GC-C-IRMS was identified according to their appearance time compared with a standard mixture composed of 26 different FAMEs. Microbial PLFA was used to reflect the biomass of living microorganisms.

The following PLFA biomarkers were used: bacterial PLFA: i15:0, a15:0, i16:0, 16:1 ω7c, i17:0, c17:0 ω7c, and c19:0 ω7c and nonspecific bacteria (14:0, 16:0, and 18:0); Fungal PLFA: 18:2 ω6c and 18:2 ω9c; gram positive PLFA: i15:0, a15:0, i16:0, and i17:0; gram negative PLFA: 16:1 ω7c, c17:0 ω7c, and c19:0 ω7c (Briar et al., 2011; Dempsey et al., 2013; Kou et al., 2020).

Amino sugars were quantified according to the method of Zhang and Amelung (1996). Briefly, after the soil samples were hydrolyzed with 6 M HCl for 8 h, the solution was filtered, adjusted to a pH of 6.6–6.8, centrifuged (2000×*g*, 10 min), and freeze-dried. Then, methanol was added to remove the amino sugars from the residues. Finally, the purified amino sugars were converted into aldononitrile derivatives and extracted with dichloromethane from the aqueous solution. After evaporating dichloromethane, the amino sugar derivatives were redissolved in the mixed hexane and ethyl acetate solvent (v:v = 1: 1) for quantification. Myo-inositol was added as an internal standard before hydrolysis, and N-methylglucamine was added before derivatization as the recovery standard. The amino sugar derivatives were separated on an Agilent 7890B GC (Agilent) equipped with an HP-5 (30 m × 0.25 mm × 0.25 μm) fused silica column and flame ionization detector. The proportion of ^{13}C incorporation of amino sugars was determined by GC/MS (Finnigan trace; Thermo Electron Finnigan Co. Ltd., USA) (He et al., 2006). The GC/MS was equipped with a quadruple MS attached chemical ionization (CI) source. Amino sugar derivatives were separated using a HP-5MS gas chromatography capillary column. High purity of helium was used as carrier gas and the flow rate was set at 0.8 mL min^{-1}. The inlet temperature was 250°C. CI source temperature was 180°C, the flow rate of CH_4 was 1.5 mL min^{-1}, and the GC/MS interface temperature was 250°C. The main fragment ions (F) and corresponding isotope fragment peaks (F + n) were detected in a full scan with a range of 40–500 mass numbers (He et al., 2006).

For fungal necromass C calculated, we subtracted bacterial GluN from total GluN first assuming that MurA and GluN occur at a 1:2 molar ratio on average in bacterial cells. Then, we multiplied fungal GluN by the averaged conversion factor of 9 to obtain fungal necromass C. Bacterial necromass C was estimated by multiplying MurA by the averaged conversion factor of 45 (Appuhn & Joergensen, 2006).

2.4 | Soil fauna analysis

Nematodes as microfauna were extracted from 100 g of fresh soil using a modified cotton-wool filter method (Liang et al., 2009) and fixed in 4% formaldehyde solution. Then, nematodes were identified to genus level using a microscope (OLYMPUS BX51) according to Bongers (1994) and Li et al. (2017). For ^{13}C enrichment analysis, the nematodes were picked using a cow eyelash by hand under a dissecting microscope (LEICA DFC290) and rinsed the body with deionized water. Each nematode then divided into the following four trophic groups by feeding habits and esophagus characteristics: bacterivores, fungivores, plant parasites, and omnivores–predators (Yeates, 2003). The mean dry weight of each nematode sample ranged from 11 to 100 μg. Thus at least the 100 bacterivorous individuals, 150 fungivorous individuals, 100 plant-parasitic individuals, and 40 predator–omnivore individuals were used to determine ^{13}C. If the expected weight did not reach, the picking process would be repeated until getting the weight for determination. Then they were placed in tin capsules (11 × 6 mm) and dried for 2 days at 60°C. The nematode analysis was conducted using an elemental analyzer (Flash Elemental Analyzer 1112) with a stable isotope ratio mass spectrometer interfaced (Thermo Finnigan, DELTA Plux XP). The Elemental Analyzer (EA) with smaller oxidation and reduction reactor tubes was used to allow lower carrier gas flow and increased the sensitivity of determination (Langel & Dyckmans, 2014; Pausch et al., 2016).

Soil mesofauna (mainly including Acarina, Collembola, and Enchytraeidae) was extracted from 100 g of fresh soil using a Tullgren funnel extractor (Burkard Mfg. Co. Ltd) for 48 h, and collected in 75% alcohol solution. For ^{13}C enrichment analysis, the mesofauna were determined to order level (Yin, 2000a, 2000b) and hand-picked using a cow eyelash under a dissecting microscope (LEICA DFC290), placed in tin capsules (11 × 6 mm) and dried for 2 days at 60°C. Mean weight of each sample ranged from 70 to 500 μg, and an elemental analyzer (Flash EA 1112) with a stable isotope ratio mass spectrometer interfaced was used to analyze the ^{13}C incorporation into mesofauna communities (Thermo Finnigan, DELTA Plux XP).

2.5 | Calculations

The ^{13}C enrichment of individual PLFA was corrected by the measured ^{13}C enrichment of corresponding FAME using the following equation (Abraham et al., 1998; Tavi et al., 2013):

$$n_{cd}\,{}^{13}C\ \text{atom}\%_{cd} = n_c\,{}^{13}C\ \text{atom}\%_c + n_d\,{}^{13}C\ \text{atom}\%_d,$$

where $^{13}C\ \text{atom}\%_{cd}$ is the ^{13}C enrichment of the PLFA, $^{13}C\ \text{atom}\%_c$ is the ^{13}C enrichment of the FAME, and $^{13}C\ \text{atom}\%_d$ is the ^{13}C enrichment of the methanol for methylation. The n is the carbon numbers in the PLFA, and n_c, n_d, and n_{cd}, are the carbon numbers of underivatized compounds, derivatized compounds (methanol, $n_d = 1$) and corresponding derivatized compounds, respectively.

The carbon fraction derived from the straw in all carbon pools (SOC, POC, MAOC, PLFA carbon, nematode biomass carbon, and mesofauna biomass carbon) (f) was calculated according to de Troyer et al. (2011) and Bradford et al. (2012):

$$f = (^{13}C\ \text{atom}\%_{\text{sample}} - {}^{13}C\ \text{atom}\%_{\text{control}}) \times 100 \Big/ (^{13}C\ \text{atom}\%_{\text{residue}} - {}^{13}C\ \text{atom}\%_{\text{control}}),$$

where the $^{13}C\ \text{atom}\%_{\text{sample}}$ and $^{13}C\ \text{atom}\%_{\text{control}}$ refer to the ^{13}C enrichment with and without straw addition, respectively, and $^{13}C\ \text{atom}\%_{\text{residue}}$ (96 atom%) is the ^{13}C enrichment of the initial residue material.

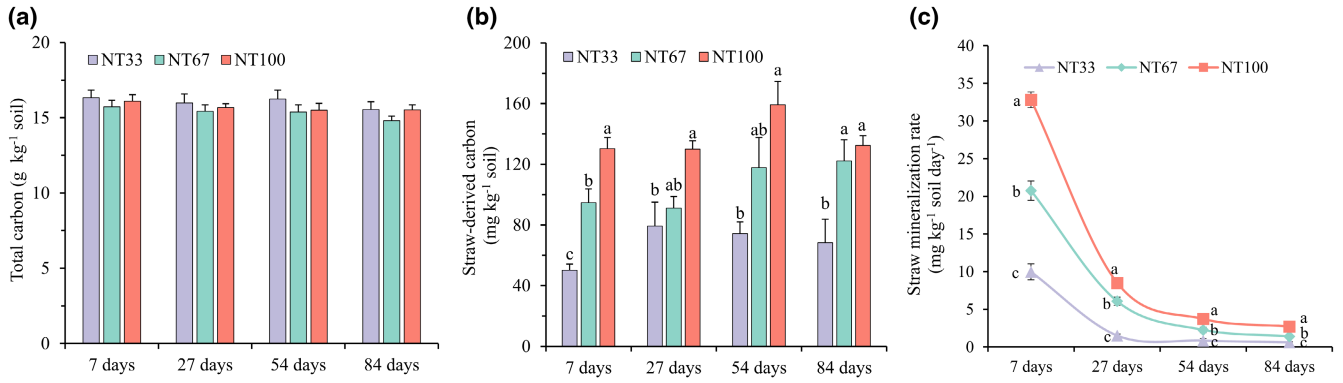

FIGURE 2 Total carbon, straw-derived carbon, and straw mineralization rate in different straw mulching treatments at the four sampling stages. Different lower-case letters represent significant differences at $p < .05$ among treatments at the same sampling stage as determined by a Tukey's post-hoc test. NT33, NT67, and NT100 represent no-tillage with 33%, 67%, and 100% straw mulching every year, respectively. [Colour figure can be viewed at wileyonlinelibrary.com]

The amount of straw carbon incorporated into a given fraction ($C_{derived}$) was calculated with the following equation (Blaud et al., 2012):

$$C_{derived} = C_{pool} \times f / 100,$$

where C_{pool} is the amount of carbon in the different pools (i.e., the total SOC, POC, MAOC, PLFA carbon, nematode carbon, and mesofauna carbon pools).

Relative turnover rates of the single organism carbon pools were calculated by dividing the net tracer incorporation by the pool size (Pausch et al., 2016).

$$r(C_P)_F = 100 \times n(C_P)_F / n(C_T)_F,$$

where the percentage of a certain carbon pool ($r(C_P)_F$, %) was calculated as the ratio of the ^{13}C stock of the respective biological pool ($n(C_P)_F$, ng g^{-1}) (i.e., the $SO^{13}C$, PLFA ^{13}C, nematode ^{13}C, or mesofauna ^{13}C pools) to the total carbon stocks of each pool ($n(C_T)_F$, ng g^{-1}).

The proportion of straw C mineralization ($M_{residue}$) was calculated as follows (Xu et al., 2019):

$$M_{residue} = \left(1 - \left(F_{residue} \times C_{total}\right) / C_{residue}\right),$$

where C_{total} is the amount of total soil carbon in the straw treatment, $C_{residue}$ is the amount of initial C (g) of the straw, and $F_{residue}$ is the proportions of remaining straw-derived C.

The relative percentage ^{13}C concentration derived from the straw was calculated with the following equation:

$$P_{(residue\ derived)} = C_{derived} / C_{residue},$$

where $C_{derived}$ was the ^{13}C amount of straw carbon incorporated into a given fraction, and the $C_{residue}$ was the ^{13}C content of straw application of different treatments.

2.6 | Statistical analysis

All statistical analysis was conducted using SPSS19 statistical software (SPSS Inc.). The effect of straw mulching amount and incubation time on microbial ^{13}C, microbial necromass ^{13}C, nematode ^{13}C and mesofauna ^{13}C were analyzed using two-way ANOVA. Differences at the $p < .05$ level were considered statistically significant. A Tukey's HSD test was used if the main effect was significant. The correlations between new carbon, microbial necromass, and different components of soil food web were analyzed using the "Corrplot" function in R software (version 3.6.2). The aggregated boosted tree (ABT) analysis was performed to quantify the relative effect of different components of soil food web on the straw-derived carbon using the "gbmplus" package with 500 trees for boosting in R software (version 2.7.1) (De'ath, 2007; Wang et al., 2020).

To explore the trophic cascade effect and anabolism effect within soil food web on straw-derived carbon, a piecewise structural equation model (piecewise SEM) was constructed under the piecewise SEM package (Lefcheck, 2016; Liu et al., 2020) and was assessed by P-value and AIC. The SEM was based on our predictions and literature review (Grace, 2006; Shipley, 2000) and the interactions among different trophic levels in the soil food web were assessed by χ^2 value, degrees of freedom (df), goodness-of-fit (GFI), and modification indices to judge the model. Structural equation modeling analysis was conducted using the Amos 17.0 software (Arbuckle, 2006).

3 | RESULTS

3.1 | Incorporation of straw-derived carbon into soil and soil food web

We found that the straw-derived $SO^{13}C$ and residue mineralization rate all showed an obvious difference among mulching treatments throughout the incubation time with the highest value found in

NT100 treatment (Figure 2b), however, the total carbon in soil was still not significantly influenced (Figure A2). The straw mineralization rate (Figure 2c) and soil respiration rate (Figure A3) showed a decreasing trend during the whole incubation time. The value of $MAO^{13}C$ has no significant difference among treatments at the incubation time of 7 and 27 days, however, a significant difference was observed at the incubation time of 54 and 84 days with the lowest value found in NT33 treatment. The proportion of $MAO^{13}C$ to $PO^{13}C$ in NT67 and NT100 treatments was significantly higher than that in NT33 treatment at the incubation time of 54 and 84 days ($p < .05$) (Figure 3). The relative percentage ^{13}C concentration of microbial PLFA (Figure 4a,b) and fungal necromass (Figure 4d) derived from the straw were significantly influenced by the mulching amount during the whole incubation time ($p < .05$). Significant differences in bacterial and fungal ^{13}C PLFA were only found in 54 and 84 days (Figure 4a,b), with the highest values observed in NT33 treatment. The relative percentage ^{13}C concentration in fungivores has the similar trend, which corresponded to the changes of fungi (Figure 4f). The interactions of straw mulching amount and incubation time on microbial necromass were significant ($p < .05$) (Tables A2 and A3), while no significant effect was found on the mesofauna community (Table A3).

3.2 | Correlation among soil food web, microbial necromass, and soil new carbon

Aggregated boosted tree (ABT) analysis was employed to interpret the relative importance of soil food web on the straw-derived carbon. Fungal necromass (28.17%), fungi (21.63%), and bacteria (16.71%) were identified as primary factors associated with the changes of new carbon (Figure 5b). The total relative importance of microbial necromass on the straw-derived carbon reached 32.0%. Soil carbon turnover rate was significantly correlated with the turnover rate of microbial and its necromass (Figure 5a). The straw-derived carbon of fungi also positively correlated with that of fungivores ($p < .05$) (Figure A1). The piecewise SEM provided a good fit to the data for the contribution of both predation and anabolism effect (AIC = 12.00, $p > .05$) (Figure 5d). Specially, compared with the predation and bacterial anabolism effect, the fungal anabolism effect made a significant positive contribution to the soil new carbon formation (Figure 5c,d).

3.3 | The control of soil food web over the soil carbon sequestration

The SEM was used to identify the pathways mediating the contribution of soil food web to SOC sequestration under the exogenous straw input condition. The SEM provided a good fit to the data (χ^2/df = 0.865, $p = .616$, GFI = 0.953), and explaining 62% and 29% of variation for native SOC and the SOC derived from straw, respectively (Figure 6). Based on the SEM, a significant positive correlation between bacteria and bacterial necromass, or between fungi and fungal necromass was proved. Microbial community rather than higher trophic levels within soil food web, exerts a direct and dominant effect on the native SOC decomposition and the new SOC formation ($p < .05$). Although there was a strong trophic interactions and carbon transformation within soil food web, the overall effect of predation eventually made an indirect contribution to native SOC decomposition (BOX 3) and new SOC formation (BOX 4), which was reflected by the correlation between soil microbes and soil fauna (BOXES 1 and 2) (Figure 6).

4 | DISCUSSION

Soil ecosystems have some resilience and regulation capacity to keep itself in balance. In other words, the SOC was not increased continuously with the increasing straw input in our study (Figure A2), which showed that only the "renewal effect" occurred after the saturation point is reached (Dupont et al., 2009; Kou et al., 2020), and a renewal process of soil carbon was formed. In this regard, we revealed how this renewal process occurred, especially the role of soil food web in the microbial carbon pump was quantified by isotopic tracing. We found that the different amounts of straw application had

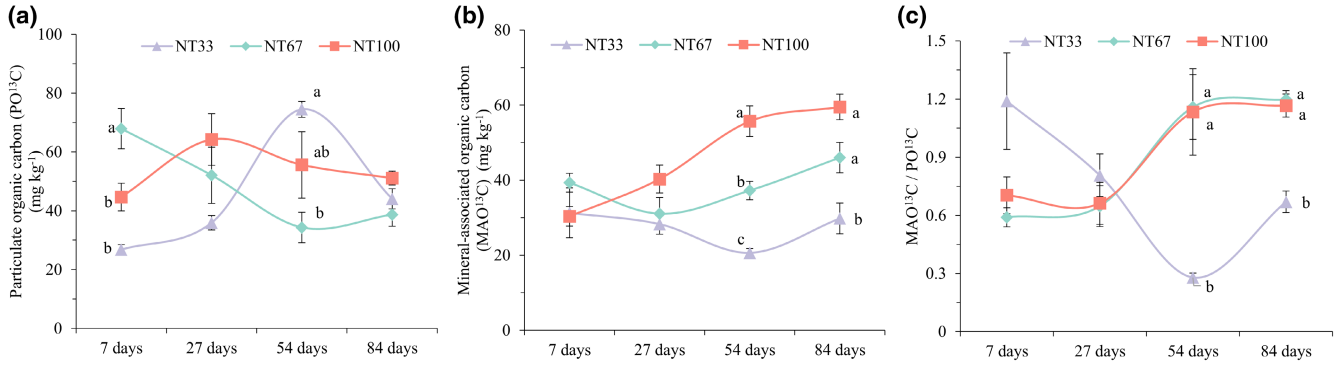

FIGURE 3 $PO^{13}C$, $MAO^{13}C$, and their proportion in different straw mulching treatments at the four sampling stages. Different lower-case letters represent significant differences at $p < .05$ among treatments at the same sampling stage as determined by a Tukey's post-hoc test. NT33, NT67, and NT100 represent no-tillage with 33%, 67%, and 100% straw mulching every year, respectively. [Colour figure can be viewed at wileyonlinelibrary.com]

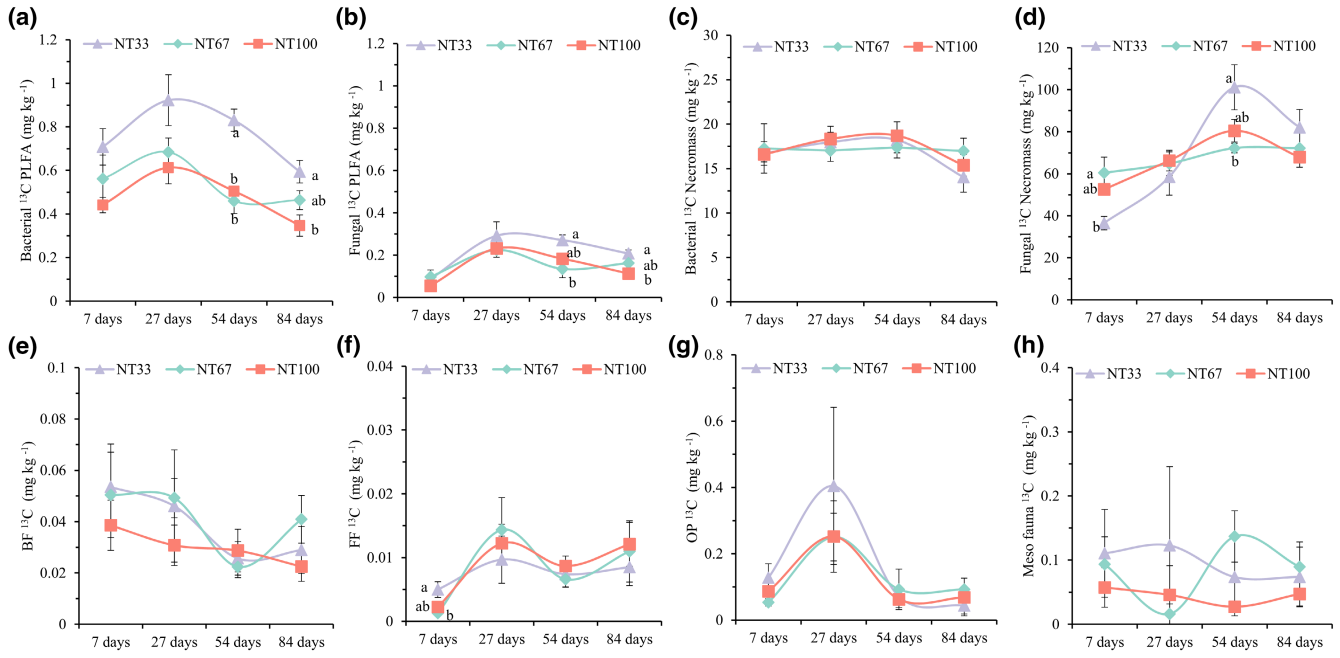

FIGURE 4 The relative ^{13}C concentration derived from residue of different components within soil food webs at the four sampling stages. Different lower-case letters represent significant differences at $p < .05$ among treatments at the same sampling stage as determined by a Tukey's post-hoc test. BF, bacterivores nematode; FF, fungivores nematode; OP, omnivores–predator nematode. [Colour figure can be viewed at wileyonlinelibrary.com]

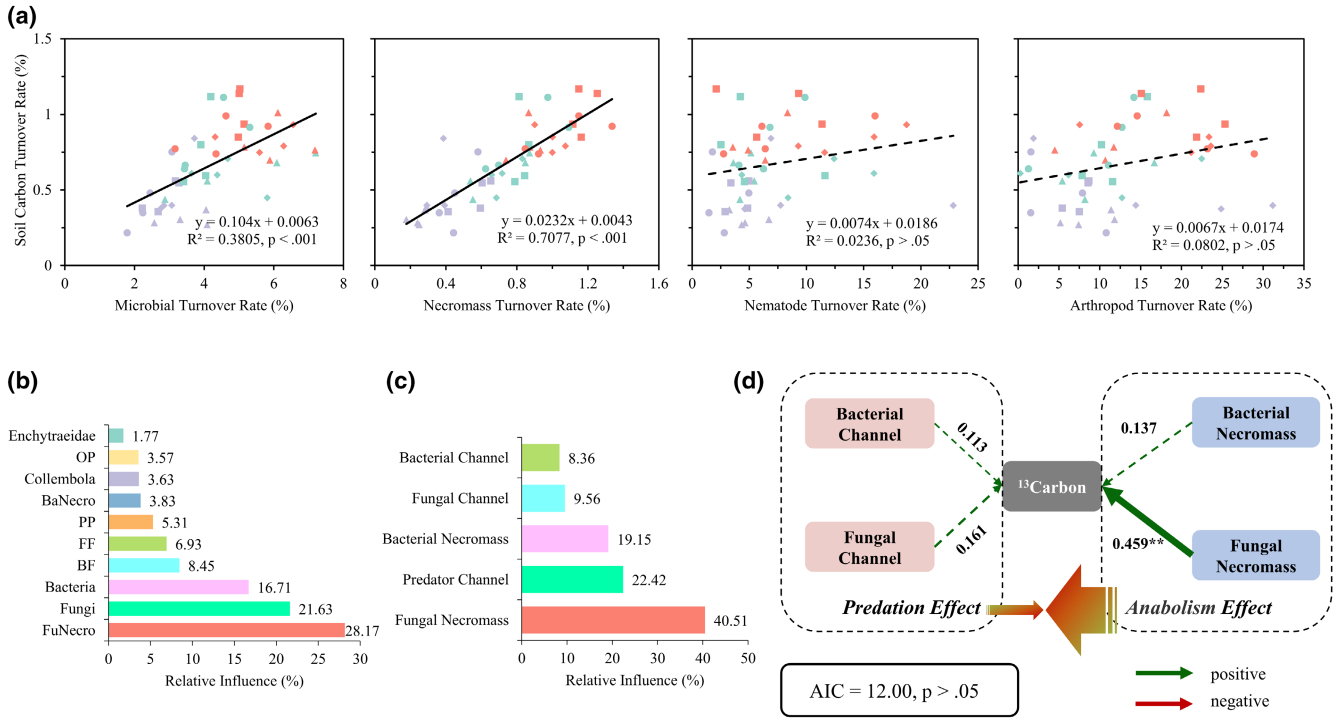

FIGURE 5 Relationship between soil carbon turnover rate and different components turnover rates in soil food web (a), the aggregated boosted tree (ABT) analysis showed the relative effect of soil fauna (b) and energy channels (c) on the new carbon, and piecewise structural equation modeling of anabolism and predation effect on the new carbon (d). BF, bacterivores nematode; FF, fungivores nematode; PP, plant parasites nematode; OP, omnivores–predator nematode. [Colour figure can be viewed at wileyonlinelibrary.com]

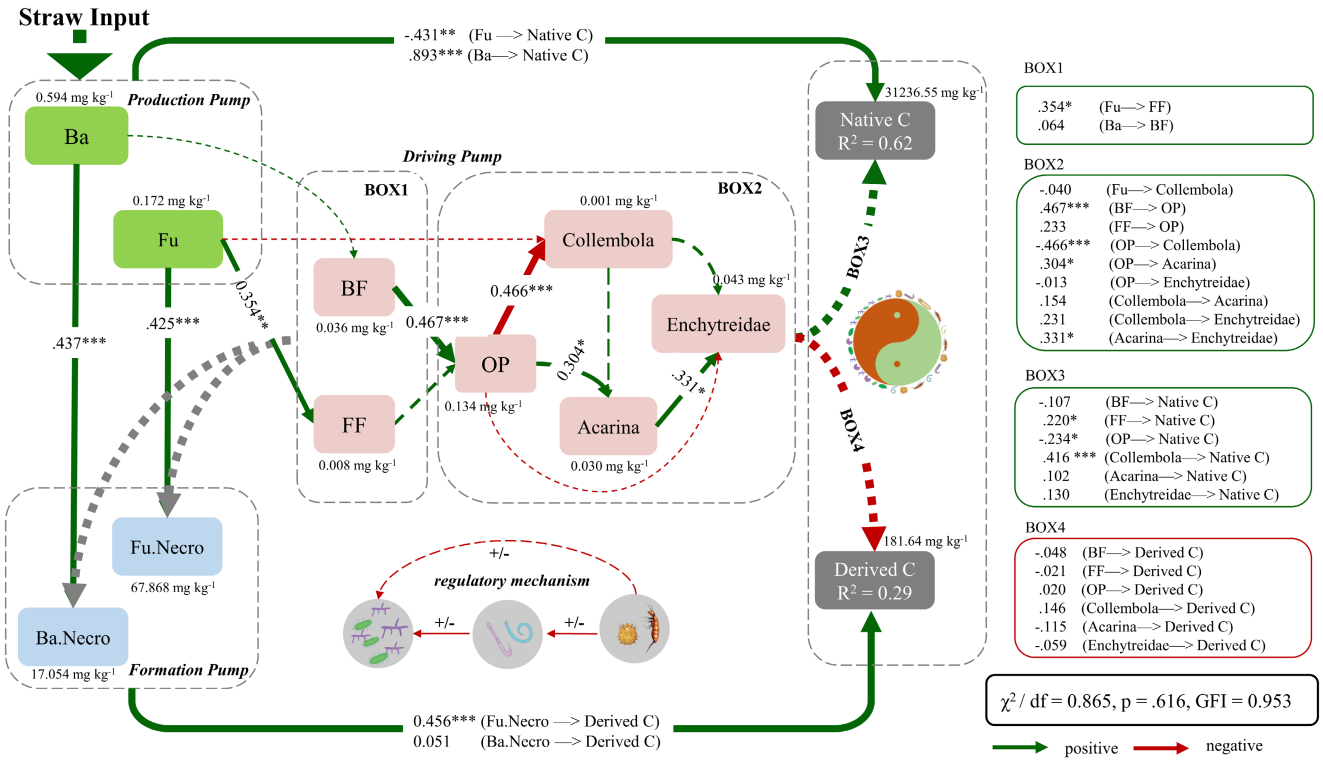

FIGURE 6 Structure equation modeling to explore the soil food web control over the soil carbon storage process. Numbers next to the arrows are the standardized path coefficients. The width of the arrows indicates the strength of the causal influence. Percentages close to endogenous variables indicate the variance explained by the model. Ba, bacteria; BaNecro, bacterial necromass; FuNecro, fungal necromass; BF, bacterivores nematode; FF, fungivores nematode; Fu, fungi; OP, omnivores–predator nematode; PP, plant parasites nematode. [Colour figure can be viewed at wileyonlinelibrary.com]

no significant effect on the total amount of SOC. However, there were significant differences in the fraction of straw-derived $SO^{13}C$ ("new" carbon, including the $PO^{13}C$ and $MAO^{13}C$) among different straw amount treatments. Additionally, our study found that the proportion of MAOC relative to POC increased with straw input amount. It is well known that two components (POC vs. MAOC) of the SOC pool are very different in terms of their formation, persistence, and functioning (Cotrufo et al., 2013; Lavallee et al., 2020). MAOC, on average, persists longer than POC, and considers as more stable SOC (Tang et al., 2023). Previous Microbial Efficiency-Matrix Stabilization (MEMS) framework also pointed out that plant constituents were the dominant source of microbial products, and these microbial products of decomposition would thus become the main precursors of a stable SOC pool (Cotrufo et al., 2013). So, although the total amount of SOC did not differ, its component has been changed, and the "renewal effect" driven by the soil food web promotes the more stable SOC. The soil food web showed a "seemingly peaceful surface but actual undercurrent" scene in our study. Notably, this phenomenon provides the evidence that the renewal process of SOC really existed and the soil food web participated and played an irreplaceable role in the renewal process.

The ABT analysis was then employed to interpret the relative importance of different soil organisms in soil food web to the "new" SOC. In this regard, we proposed that soil microbes are therefore the main executor of SOC renewal and formation. Furthermore, our study indicated that microbial necromass can make a greater contribution to SOC sequestration than previously thought (Liang et al., 2019; Zheng et al., 2021; Zhu et al., 2020). Fungal ^{13}C necromass changed with the incubation time (Figure 4d), which revealed that the entombed fungi-derived carbon is constantly being renewed and accumulated. There is difference in cell wall composition between bacteria and fungi, which affects their necromass contribution to soil carbon pool. The cell wall of bacteria is mainly composed of easily decomposable substances (such as peptidoglycan), but that of fungi is composed of relatively difficultly decomposable substances (such as chitin) (Zheng et al., 2023). Therefore, fungal necromass was the largest contributor to C sequestration via the mineral-associated SOC fraction (Luo et al., 2021). We speculated that the fungal community is the key factor affecting the carbon renewal and stability in the saturated SOC pool. However, higher trophic fauna did not show a direct contribution to the formation of soil "new" carbon (Figure 5a), but indirectly acted as the driving force of carbon flow and turnover.

Finally, we attempted to demonstrate the dynamic conversion relationship between the biological carbon turnover and the carbon sequestration within soil food web. Our SEM revealed that the microbial entombing effect from microbial necromass has a direct effect on soil carbon renewal process, whereas certain soil fauna groups tended to indirectly regulate soil carbon through mediating microbial anabolism or turnover rates. In other words, even if soil

fauna groups obtained the new carbon input by predation, it will be inevitably decomposed by microorganisms after their individual death (Thakur & Geisen, 2019) and strengthen the formation of microbial necromass to accelerate soil carbon renewal. Thus "new" carbon attained by soil fauna was fixed again through a series of biological transformation processes. We preferred to regard the predators within soil food web as the "temporary storage container" of the new carbon. Therefore, the carbon obtained by the predation process is unstable due to uninterrupted transmission to higher trophic levels and needs to be converted into a stable biological carbon pool, such as biotic necromass, which contributed to the stabilization of SOC.

Overall, we divided the regulation pump system within soil food web into three parts in SEM, that is, production pump, driving pump, and formation pump (Figure 6). Bacterial and fungal communities constitute "production pump," which dominated the decomposition process of exogenous organic carbon by anabolism, and made it into the "assembly line" of the new soil carbon. "Driving pump," mainly included the higher trophic levels of the soil food web, which preferred to accelerate the microbial anabolism or turnover rate by trophic cascading effect. "Formation pump" was composed of bacterial and fungal necromass, in which microbial communities contributed to new soil carbon via accumulating anabolism-induced necromass. Within the overall processes, microbial-derived carbon is ubiquitous and relatively stable against decomposition when it becomes physically protected by microbial entombing effect. Hence, exogenous carbon flowing through the higher trophic levels will finally contribute to the renewed carbon pool with the help of anabolism and entombing effect of microorganisms. These processes realized the transformation from unstable biological carbon pool (in vivo) to stable biological carbon pool (microbial necromass), and are considered as an important biological process for SOC renewal. Therefore, although the amount of exogenous organic matter input did not actually increase the "peaceful" amount of SOC, however, the SOC components varied and the stability was strengthened due to the "renewal" process mediated by soil food web.

It should be mentioned that other variables, such as soil respiration is necessary to be further explored to characterize the carbon use efficiency of microorganisms for revealing a complete carbon budget. The effective determination method on soil fauna necromass should be established and strengthened in further studies, how they are decomposed by microorganisms and ultimately contribute to SOC in the form of microbial necromass can be quantified, which is worth further testing. Furthermore, we certify the ^{13}C labeled microbial necromass goes up during 84 days in this study, but there is already a hint that it might go down after the straw was almost completely decomposed. Therefore, it is necessary to further certify the longer-term effect in the field condition. Nevertheless, we point out that the renewal process was closely related to the soil food web. Further studies are needed to reveal more detailed linkages between soil food webs and MCP, and their impact on ecosystem carbon sequestration in the scenario of climate change.

AUTHOR CONTRIBUTIONS

Xiaoke Zhang, Qi Li and Chao Liang designed the study; Xinchang Kou conducted the incubation experiment, soil fauna isotopic measurement, and data analysis; Yijia Tian conducted soil carbon and respiration analysis; Caiyan Lu conducted the amino sugars analysis; Hongtu Xie maintained the field experiment; Xinchang Kou, Xiaoke Zhang and Qi Li wrote the manuscript; and Elly Morriën, Wenju Liang, and Chao Liang revised the manuscript. All authors contributed to manuscript writing and reviewed the manuscript.

ACKNOWLEDGMENTS

This research was supported by the National Key Research and Development Plan, China (2022YFD1500202, 2022YFD1500601), the Strategic Priority Research Program of the Chinese Academy of Sciences (XDA28020202, XDA28010102), the National Natural Science Foundation of China (U22A20501, 41977054), the Science and Technology Research Project of the Education Department of Jilin Province (JJKH20221164KJ), the K.C. Wong Education Foundation (GJTD-2019-10), and the Major Program of Institute of Applied Ecology, Chinese Academy of Science (IAEMP202201). We are grateful to the Conservation Tillage Research and Development Station of the Chinese Academy of Sciences for providing the experimental sites. We thank M. Francesca Cotrufo and two anonymous reviewers for providing useful comments on this paper.

CONFLICT OF INTEREST STATEMENT

The authors declare that they have no known competing financial interests or personal relationships that could influence the work reported in this paper.

DATA AVAILABILITY STATEMENT

The data that support the findings of this study are available from Dryad at https://doi.org/10.5061/dryad.mgqnk9949.

ORCID

Xiaoke Zhang https://orcid.org/0000-0002-5277-2315
Qi Li https://orcid.org/0000-0002-8652-8396
Chao Liang https://orcid.org/0000-0002-9089-6546

REFERENCES

Abraham, W. R., Hesse, C., & Pelz, O. (1998). Ratios of carbon isotopes in microbial lipids as an indicator of substrate usage. *Applied and Environmental Microbiology*, *64*(11), 4202–4209. https://doi.org/10.1128/AEM.64.11.4202-4209.1998

Angst, G., Frouz, J., van Groenigen, J. W., Scheu, S., Kögel-Knabner, I., & Eisenhauer, N. (2022). Earthworms as catalysts in the formation and stabilization of soil microbial necromass. *Global Change Biology*, *28*, 4775–4782. https://doi.org/10.1111/gcb.16208

Appuhn, A., & Joergensen, R. (2006). Microbial colonisation of roots as a function of plant species. *Soil Biology and Biochemistry*, *38*(5), 1040–1051. https://doi.org/10.1016/j.soilbio.2005.09.002

Arbuckle, J. L. (2006). *Amos* (version 7.0) [computer program]. SPSS.

Bardgett, R. D., & Wardle, D. A. (2010). *Aboveground-belowground linkages*. Oxford University Press.

Bhattacharyya, S. S., Leite, F. F. G. D., France, C. L., Adekoya, A. O., Ros, G. H., de Vries, W., Melchor-Martínez, E. M., Lqbal, H. M. N., & Parra-Saldívar, R. (2022). Soil carbon sequestration, greenhouse gas emissions, and water pollution under different tillage practices. *Science of the Total Environment*, *826*, 154161. https://doi.org/10.1016/j.scitotenv.2022.154161

Blaud, A., Lerch, T., Chevallier, T., Nunan, N., Chenu, C., & Brauman, A. (2012). Dynamics of bacterial communities in relation to soil aggregate formation during the decomposition of ^{13}C-labelled rice straw. *Applied Soil Ecology*, *53*, 1–9. https://doi.org/10.1016/j.apsoil.2011.11.005

Bongers, T. (1994). De Nematoden van Nederland. In H. D. van Bohemen, D. A. G. Buizer, & A. Little (Eds.), *Vormgeving en technische realisatie* (pp. 1–386). Uitgeverij Pirola.

Bossio, D. A., Scow, K. M., Gunapala, N., & Graham, K. J. (1998). Determinants of soil microbial communities: Effects of agricultural management, season, and soil type on phospholipid fatty acid profiles. *Microbial Ecology*, *36*, 1–12. https://doi.org/10.1007/s002489900087

Bradford, M. A., Strickland, M. S., DeVore, J. L., & Maerz, J. C. (2012). Root carbon flow from an invasive plant to belowground foodwebs. *Plant and Soil*, *359*, 233–244. https://doi.org/10.1007/s11104-012-1210-y

Bradford, M. A., Wieder, W. R., Bonan, G. B., Fierer, N., Raymond, P. A., & Crowther, T. W. (2016). Managing uncertainty in soil carbon feedbacks to climate change. *Nature Climate Change*, *6*, 751–758. https://doi.org/10.1038/nclimate3071

Briar, S. S., Fonte, S. J., Park, I., Six, J., Scow, K., & Ferris, H. (2011). The distribution of nematodes and soil microbial communities across soil aggregate fractions and farm management systems. *Soil Biology and Biochemistry*, *43*(5), 905–914. https://doi.org/10.1016/j.soilbio.2010.12.017

Cotrufo, M. F., Ranalli, M. G., Haddix, M. L., Six, J., & Lugato, E. (2019). Soil carbon storage informed by particulate and mineral-associated organic matter. *Nature Geoscience*, *12*(12), 989–994. https://doi.org/10.1038/s41561-019-0484-6

Cotrufo, M. F., Wallenstein, M. D., Boot, C. M., Denef, K., & Paul, E. (2013). The microbial efficiency-matrix stabilization (MEMS) framework integrates plant litter decomposition with soil organic matter stabilization: Do labile plant inputs form stable soil organic matter? *Global Change Biology*, *19*(4), 988–995. https://doi.org/10.1111/gcb.12113

Crowther, T. W., Thomas, S. M., Maynard, D. S., Baldrian, P., Covey, K., Frey, S. D., van Diepen, L. T., & Bradford, M. A. (2015). Biotic interactions mediate soil microbial feedbacks to climate change. *Proceedings of the National Academy of Sciences of the United States of America*, *112*(22), 7033–7038. https://doi.org/10.1073/pnas.1502956112

de Castro, F., Adl, S. M., Allesina, S., Bardgett, R. D., Bolger, T., Dalzell, J. J., Emmerson, M., Fleming, T., Garlaschelli, D., Grilli, J., Hannula, S. E., de Vries, F., Lindo, Z., Maule, A. G., Öpik, M., Rillig, M. C., Veresoglou, S. D., Wall, D. H., & Caruso, T. (2021). Local stability properties of complex, species-rich soil food webs with functional block structure. *Ecology and Evolution*, *11*, 16070–16081. https://doi.org/10.1002/ece3.8278

de Troyer, I., Amery, F., van Moorleghem, C., Smolders, E., & Merckx, R. (2011). Tracing the source and fate of dissolved organic matter in soil after incorporation of a ^{13}C labelled residue: A batch incubation study. *Soil Biology and Biochemistry*, *43*(3), 513–519. https://doi.org/10.1016/j.soilbio.2010.11.016

De'ath, G. (2007). Boosted trees for ecological modeling and prediction. *Ecology*, *88*(1), 243–251. https://doi.org/10.1890/0012-9658(2007)88[243:btfema]2.0.co;2

Dempsey, M. A., Fisk, M. C., Yavitt, J. B., Fahey, T. J., & Balser, T. C. (2013). Exotic earthworms alter soil microbial community composition and function. *Soil Biology and Biochemistry*, *67*, 263–270. https://doi.org/10.1016/j.soilbio.2013.09.009

Domeignoz-Horta, L., Pold, G., Allen Liu, X. J., Frey, S. D., Melillo, J. M., & DeAngelis, K. M. (2020). Microbial diversity drives carbon use efficiency in a model soil. *Nature Communications*, *11*, 3684. https://doi.org/10.1038/s41467-020-17502-z

Dupont, S. T., Ferris, H., & Horn, M. V. (2009). Effects of cover crop quality and quantity on nematode-based soil food webs and nutrient cycling. *Applied Soil Ecology*, *41*(2), 157–167. https://doi.org/10.1016/j.apsoil.2008.10.004

Gan, H., Liang, C., & Wickings, K. (2018). Root herbivores accelerate carbon inputs to soil and drive changes in biogeochemical processes. *Rhizosphere*, *6*, 112–115. https://doi.org/10.1016/j.rhisph.2018.06.003

Garcia-Palacios, P., Shaw, E. A., Wall, D. H., & Hattenschwiler, S. (2016). Temporal dynamics of biotic and abiotic drivers of litter decomposition. *Ecology Letters*, *19*(5), 554–563. https://doi.org/10.1111/ele.12590

Grace, J. B. (2006). *Structural equation modeling and natural systems*. Cambridge University Press.

Grandy, A. S., Wieder, W. R., Wickings, K., & Kyker-Snowman, E. (2016). Beyond microbes: Are fauna the next frontier in soil biogeochemical models? *Soil Biology and Biochemistry*, *102*, 40–44. https://doi.org/10.1016/j.soilbio.2016.08.008

He, H. B., Xie, H. T., & Zhang, X. D. (2006). A novel GC/MS technique to assess ^{15}N and ^{13}C incorporation into soil amino sugars. *Soil Biology and Biochemistry*, *38*(5), 1083–1091. https://doi.org/10.1016/j.soilbio.2005.09.007

Jackson, R. B., Lajtha, K., Crow, S. E., Hugelius, G., Kramer, M. G., & Piñeiro, G. (2017). The ecology of soil carbon: Pools, vulnerabilities, and biotic and abiotic controls. *Annual Review of Ecology, Evolution, and Systematics*, *48*, 419–445. https://doi.org/10.1146/annurev-ecolsys-112414-054234

Jiang, Y. F., Xie, H. T., & Chen, Z. W. (2021). Relationship between the amounts of surface corn Stover mulch and soil mesofauna assemblage varies with the season in cultivated areas of northeastern China. *Soil and Tillage Research*, *213*, 105091. https://doi.org/10.1016/j.still.2021.105091

Kastner, M., & Miltner, A. (2018). Chapter 5-SOM and microbes—What is left from microbial life. In P. Nannipieri & T. Hernandez (Eds.), *The future of soil carbon* (pp. 125–163). Academic Press.

Kou, X. C., Ma, N. N., Zhang, X. K., Xie, H. T., Zhang, X. D., Wu, Z. F., Liang, W. J., Li, Q., & Ferris, H. (2020). Frequency of Stover mulching but not amount regulates the decomposition pathways of soil microfoodwebs in a no-tillage system. *Soil Biology and Biochemistry*, *144*, 107789. https://doi.org/10.1016/j.soilbio.2020.107789

Langel, R., & Dyckmans, J. (2014). Combined ^{13}C and ^{15}N isotope analysis on small samples using a near-conventional elemental analyzer/isotope ratio mass spectrometer setup. *Rapid Communications in Mass Spectrometry*, *28*, 1019–1022. https://doi.org/10.1002/rcm.6878

Lavallee, J. M., Soong, J. L., & Cotrufo, M. F. (2020). Conceptualizing soil organic matter into particulate and mineral-associated forms to address global change in the 21st century. *Global Change Biology*, *26*(1), 261–273. https://doi.org/10.1111/gcb.14859

Lefcheck, J. S. (2016). PIECEWISESEM: Piecewise structural equation modelling in R for ecology, evolution, and systematics. *Methods in Ecology and Evolution*, *7*, 573–579. https://doi.org/10.1111/2041-210X.12512

Lehmann, J., Hansel, C. M., Kaiser, C., Kleber, M., Maher, K., Manzoni, S., Nunan, N., Reichstein, M., Schimel, J. P., Torn, M. S., Wieder, W.

R., & Kögel-Knabner, I. (2020). Persistence of soil organic carbon caused by functional complexity. *Nature Geoscience*, *13*, 529–534. https://doi.org/10.1038/s41561-020-0612-3

Li, Q., Liang, W. J., Zhang, X. K., & Mohammad, M. (2017). *Soil nematodes of grasslands in northern China*. Zhejiang University Press; published by Elsevier Inc, London, UK.

Liang, C. (2020). Soil microbial carbon pump: Mechanism and appraisal. *Soil Ecology Letters*, *2*, 241–254. https://doi.org/10.1007/s42832-020-0052-4

Liang, C., Amelung, W., Lehmann, J., & Kästner, M. (2019). Quantitative assessment of microbial necromass contribution to soil organic matter. *Global Change Biology*, *25*, 3578–3590. https://doi.org/10.1111/gcb.14781

Liang, C., Schimel, J. P., & Jastrow, J. D. (2017). The importance of anabolism in microbial control over soil carbon storage. *Nature Microbiology*, *2*, 17105. https://doi.org/10.1038/nmicrobiol.2017.105

Liang, W. J., Lou, Y. L., Li, Q., Zhong, S., Zhang, X. K., & Wang, J. K. (2009). Nematode faunal response to long-term application of nitrogen fertilizer and organic manure in Northeast China. *Soil Biology and Biochemistry*, *41*(5), 883–890. https://doi.org/10.1016/j.soilbio.2008.06.018

Liu, T., Yang, L. H., Hu, Z. K., Xue, J. R., Lu, Y. Y., Chen, X., Griffiths, B. S., Whalen, J. K., & Liu, M. Q. (2020). Biochar exerts negative effects on soil fauna across multiple trophic levels in a cultivated acidic soil. *Biology and Fertility of Soils*, *56*, 597–606. https://doi.org/10.1007/s00374-020-01436-1

Luo, J. M., Zhang, X. K., Kou, X. C., Xie, H. T., Bao, X. L., Mahamood, M., & Liang, W. J. (2020). Effects of residue mulching amounts on metabolic footprints based on production and respiration of soil nematodes in a long-term no-tillage system. *Land Degradation & Development*, *32*, 2383–2392. https://doi.org/10.1002/ldr.3918

Luo, Y., Xiao, M. L., Yuan, H. Z., Liang, C., Zhu, Z. K., Xu, J. M., Kuzyakov, Y., Wu, J. S., Ge, T. D., & Tang, C. X. (2021). Rice rhizodeposition promotes the build-up of organic carbon in soil via fungal necromass. *Soil Biology and Biochemistry*, *160*, 108345. https://doi.org/10.1016/j.soilbio.2021.108345

Mitchell, E., Scheer, C., Rowlings, D., Cotrufo, M. F., Conant, R. T., Friedl, J., & Grace, P. (2020). Trade-off between "new" SOC stabilization from above-ground inputs and priming of native C as determined by soil type and residue placement. *Biogeochemistry*, *149*, 221–236. https://doi.org/10.1007/s10533-020-00675-6

Ni, H. W., Jing, X. Y., Xiao, X., Zhang, N., Wang, X. Y., Sui, Y. Y., Sun, B., & Liang, Y. T. (2021). Microbial metabolism and necromass mediated fertilization effect on soil organic carbon after long-term community incubation in different climates. *ISME Journal*, *15*, 2561–2573. https://doi.org/10.1038/s41396-021-00950-w

Pausch, J., Kramer, S., Scharroba, A., Scheunemann, N., Butenschoen, O., Kandeler, E., Marhan, S., Riederer, M., Scheu, S., Kuzyakov, Y., & Ruess, L. (2016). Small but active—Pool size does not matter for carbon incorporation in below-ground food webs. *Functional Ecology*, *30*, 479–489. https://doi.org/10.1111/1365-2435.12512

Richter, A., Kern, T., Wolf, S., Struck, U., & Ruess, L. (2019). Trophic and non-trophic interactions in binary links affect carbon flow in the soil micro-food web. *Soil Biology and Biochemistry*, *135*, 237–247. https://doi.org/10.1016/j.soilbio.2019.04.010

Sackeet, T. E., Classen, A. T., & Sanders, N. J. (2010). Linking soil food web structure to above- and belowground ecosystem process: A meta-analysis. *Oikos*, *119*, 1984–1992. https://doi.org/10.1111/j.1600-0706.2010.18728.x

Schimel, J., & Schaeffer, S. M. (2012). Microbial control over carbon cycling in soil. *Frontiers in Microbiology*, *3*, 1–11. https://doi.org/10.3389/fmicb.2012.00348

Schmidt, M. W. I., Torn, M. S., Abiven, S., Dittmar, T., Guggenberger, G., Janssens, I. A., Kleber, M., Kogel-Knabner, I., Lehmann, J., Manning, D. A. C., Nannipieri, P., Rasse, D., Weiner, S., & Trumbore, S. E. (2015). Persistence of soil organic matter as an ecosystem property. *Nature*, *478*, 49–56. https://doi.org/10.1038/nature10386

Shipley, B. (2000). A new inferential test for path models based on directed acyclic graphs. *Structural Equation Modeling: A Multidisciplinary Journal*, *7*, 206–218. https://doi.org/10.1207/S15328007SEM0702_4

Soong, J. L., Vandegehuchte, M. L., Horton, A. J., Nielsen, U. N., Denef, K., Shaw, E. A., Tomasel, C. M. D., Parton, W., Wall, D. H., & Cotrufo, M. F. (2016). Soil microarthropods support ecosystem productivity and soil C accrual: Evidence from a litter decomposition study in the tallgrass prairie. *Soil Biology and Biochemistry*, *92*, 230–238. https://doi.org/10.1016/j.soilbio.2015.10.014

Stockmann, U., Adams, M. A., Crawford, J. W., Field, D. J., Henakaarchchi, N., Jenkins, M., Minasny, B., McBratney, A. B., Courcelles, V. R., Singh, K., Wheeler, I., Abbott, L., Angers, D. A., Baldock, J., Bird, M., Brookes, P. C., Chenu, C., Jastrow, J. D., Lal, R., … Zimmermann, M. (2013). The knowns, known unknowns and unknowns of sequestration of soil organic carbon. *Agriculture, Ecosystems and Environment*, *164*, 80–99. https://doi.org/10.1016/j.agee.2012.10.001

Sven, M., Reinhard, L., Ellen, K., & Stefan, S. (2007). Use of stable isotopes (^{13}C) for studying the mobilization of old soil organic carbon by endogeic earthworms (Lumbricidae). *European Journal of Soil Biology*, *43*, S201–S208. https://doi.org/10.1016/j.ejsobi.2007.08.017

Tang, B., Rocci, K. S., Lehmann, A., & Rillig, M. (2023). Nitrogen increases soil organic carbon accrual and alters its functionality. *Global Change Biology*, *29*, 1971–1983. https://doi.org/10.1111/gcb.16588

Tavi, N. M., Martikainen, P. J., Lokko, K., Kontro, M., Wild, B., Richter, A., & Biasi, C. (2013). Linking microbial community structure and allocation of plant-derived C in an organic agricultural soil using $^{13}CO_2$ pulse-chase labelling combined with ^{13}C-PLFA profiling. *Soil Biology and Biochemistry*, *58*, 207–215. https://doi.org/10.1016/j.soilbio.2012.11.013

Thakur, M. P., & Geisen, S. (2019). Trophic regulations of the soil microbiome. *Trends in Microbiology*, *27*(9), 771–780. https://doi.org/10.1016/j.tim.2019.04.008

Torri, S. I., Corrêa, R. S., & Renella, G. (2014). Soil carbon sequestration resulting from biosolids application. *Applied and Environmental Soil Science*, *2014*, 821768. https://doi.org/10.1155/2014/821768

Wang, B. R., An, S. S., Liang, C., Liu, Y., & Kuzyakov, Y. (2021). Microbial necromass as the source of soil organic carbon in global ecosystems. *Soil Biology and Biochemistry*, *162*, 108422. https://doi.org/10.1016/j.soilbio.2021.108422

Wang, C., Qu, L. R., Yang, L. M., Liu, D. W., Morrissey, E., Miao, R. H., Liu, Z. P., Wang, Q. K., Fang, Y. T., & Bai, E. (2021). Large-scale importance of microbial carbon use efficiency and necromass to soil organic carbon. *Global Change Biology*, *27*, 2039–2048. https://doi.org/10.1111/gcb.15550

Wang, J., Liu, G. B., Zhang, C., & Wang, G. L. (2020). Effect of long-term destocking on soil fungal functional groups and interactions with plants. *Plant and Soil*, *448*, 495–508. https://doi.org/10.1007/s11104-020-04452-0

Xu, Y. D., Ding, F., Gao, X. D., Wang, Y., Li, M., & Wang, J. K. (2019). Mineralization of plant residues and native soil carbon as affected by soil fertility and residue type. *Journal of Soils and Sediments*, *19*, 1407–1415. https://doi.org/10.1007/s11368-018-2152-7

Yeates, G. W. (2003). Nematodes as soil indicators: Functional and biodiversity aspects. *Biology and Fertility of Soils*, *37*, 199–210. https://doi.org/10.1007/s00374-003-0586-5

Yin, W. Y. (2000a). *Soil animals of China*. Science Press.

Yin, W. Y. (2000b). *Pictorial keys to soil animals of China*. Science Press.

Zhang, X. D., & Amelung, W. (1996). Gas chromatograph1c determination of muramic acid, glucosamine, mannosamine, and galactosamine in soils. *Soil Biology and Biochemistry*, *28*(9), 1201–1206. https://doi.org/10.1016/0038-0717(96)00117-4

Zheng, T. T., Miltner, A., Liang, C., Nowak, K. M., & Kastner, M. (2021). Turnover of gram-negative bacterial biomass-derived carbon

through the microbial food web of an agricultural soil. *Soil Biology and Biochemistry*, *152*, 108070. https://doi.org/10.1016/j.soilbio.2020.108070

Zheng, T. T., Miltner, A., Liang, C., Nowak, K. M., & Kastner, M. (2023). Turnover of bacterial biomass to soil organic matter via fungal biomass and its metabolic implications. *Soil Biology and Biochemistry*, *180*, 108995. https://doi.org/10.1016/j.soilbio.2023.108995

Zhu, E. R., Cao, Z. J., Jia, J., Liu, C. Z., Zhang, Z. H., Wang, H., Dai, G. H., He, J. S., & Feng, X. J. (2021). Inactive and inefficient: Warming and drought effect on microbial carbon processing in alpine grassland at depth. *Global Change Biology*, *27*, 2241–2253. https://doi.org/10.1111/gcb.15541

Zhu, X. F., Jackson, R. D., Delucia, E. H., Tiedje, J. M., & Liang, C. (2020). The soil microbial carbon pump: From conceptual insights to empirical assessments. *Global Change Biology*, *26*, 6032–6039. https://doi.org/10.1111/gcb.15319

SUPPORTING INFORMATION

Additional supporting information can be found online in the Supporting Information section at the end of this article.

How to cite this article: Kou, X., Morriën, E., Tian, Y., Zhang, X., Lu, C., Xie, H., Liang, W., Li, Q., & Liang, C. (2023). Exogenous carbon turnover within the soil food web strengthens soil carbon sequestration through microbial necromass accumulation. *Global Change Biology*, *29*, 4069–4080. https://doi.org/10.1111/gcb.16749